Supplementary Text, Figures, and Tables for "Effects of Increasing Aridity on Ambient Dust and Public Health in the U.S. Southwest under Climate Change"

Additional data and analysis codes are provided as supplemental files.

S1. IMPROVE data

The IMPROVE definition of "Fine Soil" relies on the mass concentrations of common soil-derived elements (aluminium, silicon, calcium, iron, and titanium) and their normal oxides, along with a correction factor to account for other species such as water and carbonate [*Malm et al.*, 1994, 2004]. However, *Hyslop et al.* [2015] discovered that changes in analytical methods between 1995 and 2010 may have introduced spurious temporal trends in aluminium, silicon, and titanium. To assure the quality of the fine dust data over the 2000-2015 timeframe, we use the iron content of filter samples as a fine dust proxy, following the approach first proposed by *Hand et al.* [2016] and subsequently updated by *Achakulwisut et al.* [2017]. Here we calculate site-specific monthly mean fine dust concentrations as follows. (1) We neglect any sites at which $PM_{2.5}$-Iron is measured below the minimum detection limit on more than 20% of all days. (2) We screen out "high-combustion" days when the elemental carbon (EC) concentration exceeds a threshold value, defined here as the 2000-2015 EC monthly mean + 1 standard deviation for a given site. (3) If at least 50% of daily data are available for a given site and month, we calculate monthly mean $PM_{2.5}$-Iron concentrations from the daily values. (4) We approximate monthly mean fine dust concentrations as 6.5% $PM_{2.5}$-Iron, based on observed linear relationships between daily $PM_{2.5}$-Iron and IMPROVE "Fine Soil" from 2011 to 2015 (Figure S9). Since 2011, a new Panalytical XRF system has been used to determine elemental concentrations at all IMPROVE sites [*Hand et al.*, 2017]. *Lawrence and Neff* [2009] demonstrated that on average globally, the concentrations of most major elements in airborne dust tend to be similar to the composition of the upper continental crust. For iron, the observed global mean value is 3.6% (range of 1.3-7.8%). (5) Finally, we screen out sites with less than 50% monthly data for the 16-year time period. On average, the analytical uncertainties associated with our calculated monthly mean fine dust values are ~0.06% using error propagation. Further details behind our choice and method in using $PM_{2.5}$-Iron as a proxy for fine dust are provided in the Supplement of Achakulwisut et al. [2017].

S2. Additional information on CMIP5 model selection in the CIRA framework

As in many sectoral impact analyses in the literature, the selection of a subset of climate models is necessary due to computational, time, and resource constraints. The six CMIP5 models used in this analysis were chosen primarily based on their ability to capture variability in temperature and precipitation in the United States. While many different metrics could be used in this type of comparison, the broader research effort, of which this work is a part, based selection on an accepted approach – comparing the projections from CMIP5 models for annual and seasonal temperature and precipitation [Martinich and Crimmins 2019].

Besides model performance, our selection criteria included model independence and broader usage by the scientific community. The CMIP5 models vary in their ability to resolve certain climate system processes, including those most relevant to the United States. In addition, while over 60 different CMIP5 models are available, a number of the models share computer code or are parametrized in similar ways. Recent studies [Sanderson et al. 2015a, 2015b; McSweeney et

al. 2015] provide analysis of both model skill at the global scale and independence of underlying code. Ultimately, we apply equal weight to each of the results derived using the six models, but we also provide the model specific results to facilitate analysts who wish to employ other weighting criteria (using, for example, Eyring et al. 2019).

With insufficient resources to conduct a country-specific weighting analysis based on skill and independence, a qualitative consideration of these metrics is still valuable. For purposes of this project, the six GCMs selected were developed by different, well-known modeling groups whose models are frequently used in the literature. In addition, three of the GCMs (CCSM4, GISS-E2-R, and GFDL-CM3) are developed by domestically-based modeling groups (NCAR, NASA, and GFDL, respectively). There is some expectation that modeling teams may pay closer attention to the regional climate in the region where the team is based, and that therefore domestically-based modeling groups might have comparatively greater skill for purposes of impacts analysis in the United States.

S3. Sensitivity analysis of the value of a statistical life (VSL) and total valuation estimates to alternative economic growth and income elasticity inputs

As outlined in the main text, we estimate the economic value of projected health burdens based on federal guidance and valuation functions included in the BenMAP-CE model. For mortality endpoints, we use a base VSL of $7.9 million ($2008) based on 1990 incomes. To create a VSL using $2015 and based on 2015 incomes, the standard value was adjusted for inflation and income growth. The resulting value, $10.0 million for 2015 ($2015), was adjusted to future years to reflect the impact of income growth on individual willingness-to-pay to reduce mortal risk over time, and to our "current climate" base year of 2010, by assuming an elasticity of VSL to GDP per capita of 0.4. The income elasticity is based on empirical evidence that indicates that VSL grows about 0.4% for each 1% increase in GDP/capita – the specific value provided in BenMAP-CE – 0.4 - reflects a literature review completed in the mid 1990s.

Recent literature provides a basis for projecting GDP/capita through our full simulation period (through 2100), and for potentially updating the income elasticity. A recent literature review suggests that income elasticity values as high as 1.0 might be more consistent with emerging literature on the topic (see for example Robinson et al. 2018) – the implication of which is that VSL would grow proportionately with GDP/capita.

The results of these sensitivity tests are presented in Table S7. The first row shows the VSL used in the estimates presented in the main text. Using a value of 1.0 for income elasticity, yields higher estimates, ranging from 16% higher in 2030 to 87% higher in 2090 than the VSL estimates used in the main text.

References

Achakulwisut, P., L. Shen, and L. J. Mickley (2017), What controls springtime fine dust variability in the western United States? Investigating the 2002-2015 increase in fine dust in the U.S. Southwest, *J. Geophys. Res. Atmos.*, *122*, doi:10.1002/2017JD027208.

Eyring, V., P.M. Cox, and M.S. Williamson (2019), Taking climate model evaluation to the next level, *Nature Climate Change*, 9:102–110.

Hand, J. L., W. H. White, K. A. Gebhart, N. P. Hyslop, T. E. Gill, and B. A. Schichtel (2016), Earlier onset of the spring fine dust season in the southwestern United States, *Geophys. Res. Lett.*, *43*, 4001–4009, doi:10.1002/2016GL068519.

Hyslop, N. P., K. Trzepla, and W. H. White (2015), Assessing the Suitability of Historical PM2.5 Element Measurements for Trend Analysis, *Environ. Sci. Technol.*, *49*(15), 9247–9255, doi:10.1021/acs.est.5b01572.

Lawrence, C. R., and J. C. Neff (2009), The contemporary physical and chemical flux of aeolian dust: A synthesis of direct measurements of dust deposition, *Chem. Geol.*, *267*(1-2), 46–63, doi:10.1016/j.chemgeo.2009.02.005.

Malm, W. C., J. F. Sisler, D. Huffman, R. A. Eldred, and T. A. Cahill (1994), Spatial and seasonal trends in particle concentration and optical extinction in the United States, *J. Geophys. Res.*, *99*(D1), 1347–1370, doi:10.1029/93JD02916.

Malm, W. C., B. A. Schichtel, M. L. Pitchford, L. L. Ashbaugh, and R. A. Eldred (2004), Spatial and monthly trends in speciated fine particle concentration in the United States, *J. Geophys. Res.*, *109*(D3), D03306, doi:10.1029/2003JD003739.

Martinich, J. and A. Crimmins (2019), Climate damages and adaptation potential across diverse U.S. sectors. *Nature Climate Change* (in press).

McSweeney, C.F., R.G. Jones, and D.P. Rowell (2015), Selecting CMIP5 GCMs for downscaling over multiple regions. *Clim Dyn* 44, 3237-3260 (2015).

Robinson, Lisa A., James K. Hammitt, and Lucy O'Keeffe (2018), Valuing Mortality Risk Reductions in Global Benefit-Cost Analysis. Guidelines for Benefit-Cost Analysis Project, Working Paper No. 7. Prepared for the Benefit-Cost Analysis Reference Case Guidance Project, funded by the Bill and Melinda Gates Foundation. March 2018. Available at https://cdn2.sph.harvard.edu/wp-content/uploads/sites/94/2017/01/Robinson-Hammitt-OKeeffe-VSL.2018.03.23.pdf

Sanderson, B., R. Knutti, and P. Caldwell (2015a), A representative democracy to reduce interdependency in a multimodel ensemble. *J Clim* 28, 5171-5194 (2015).

Sanderson, B., R. Knutti, and P. Caldwell (2015b), Addressing interdependency in a multi-model ensemble by interpolation of model properties. *J of Clim* 28, 5150-5170 (2015).

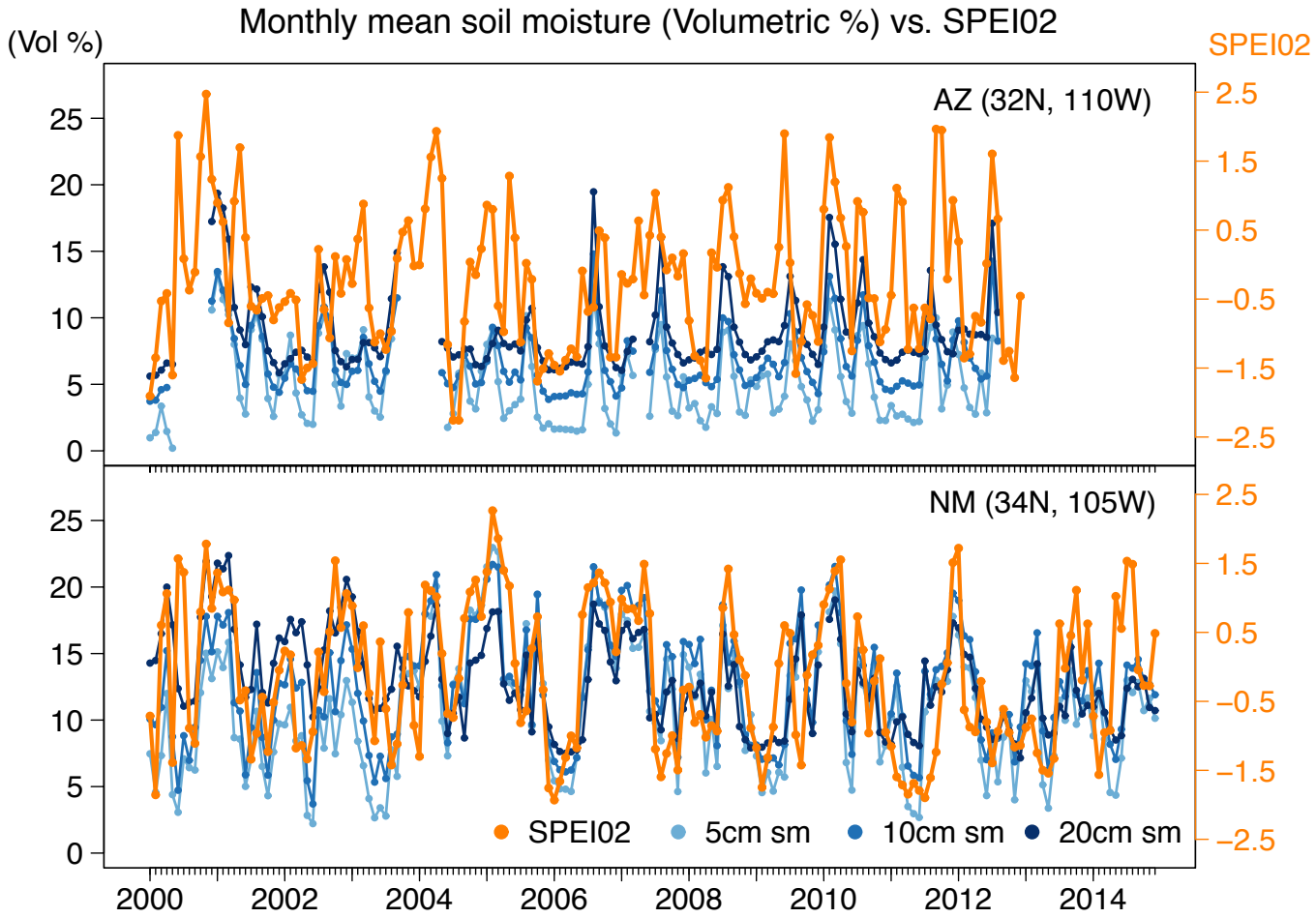

Figure S1. Timeseries of 2000-2014 monthly mean SPEI02 and soil moisture (volumetric %) at one site in Arizona (site #2026) and another in New Mexico (site #2015), using soil moisture measurements from the Soil Climate Analysis Network (SCAN). The orange line shows SPEI02, and the blue lines show soil moisture measured at 5, 10, and 20 cm depths. The statistically significant correlations ($p < 0.05$) between SPEI02 and soil moisture range from 0.40-0.48 for the Arizona site, and 0.56-0.59 for the New Mexico site, depending on the soil depth. (This Figure is replicated from A2018, Figure S4.)

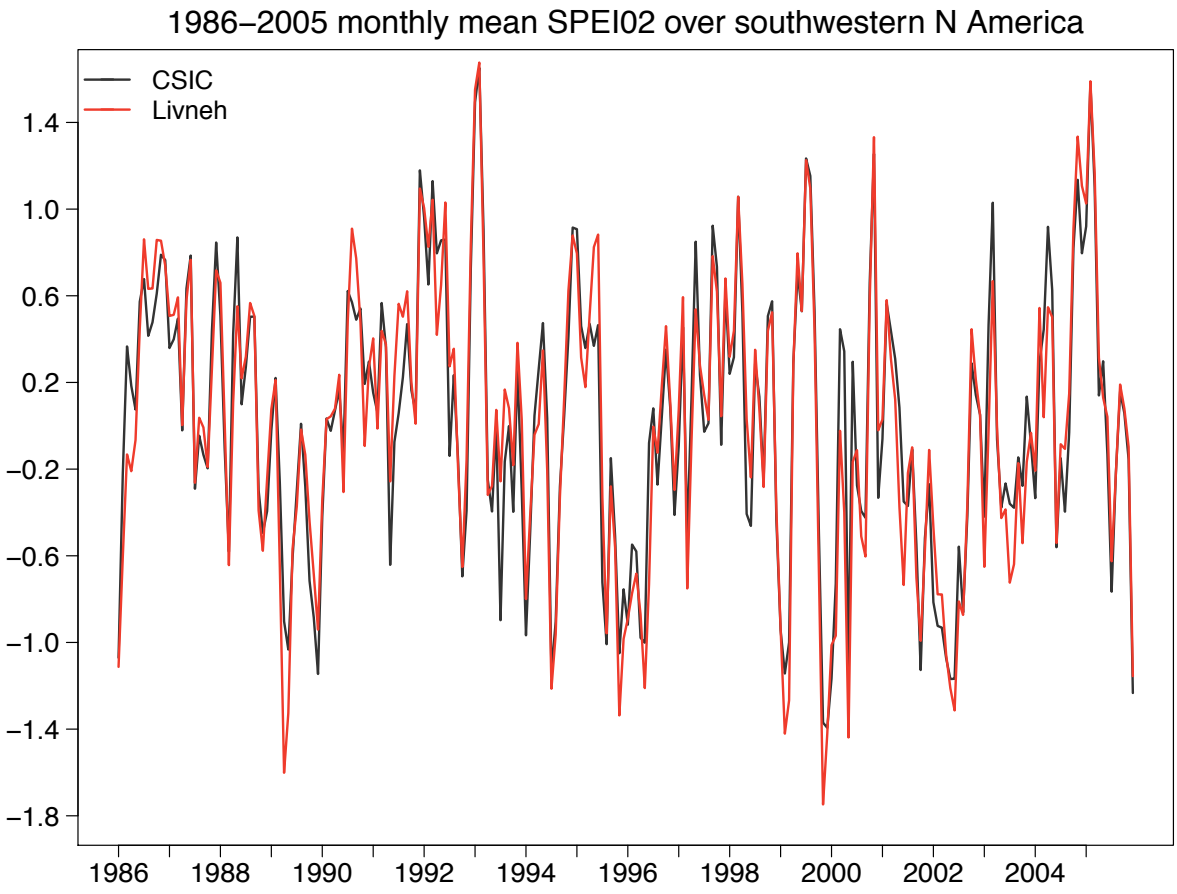

Figure S2. 1986-2005 monthly mean SPEI02 averaged over 117°-103°W, 28°-40°N from the Spanish National Research Council (CSIC, black line), which calculates PET using the FAO Penman-Monteith equation versus those calculated from Livneh et al. [2015] meteorological data using the Modified-Hargreaves PET equation (red line). The two time series have a significant linear correlation ($r = 0.95$, $p = 2.2 \times 10^{-16}$).

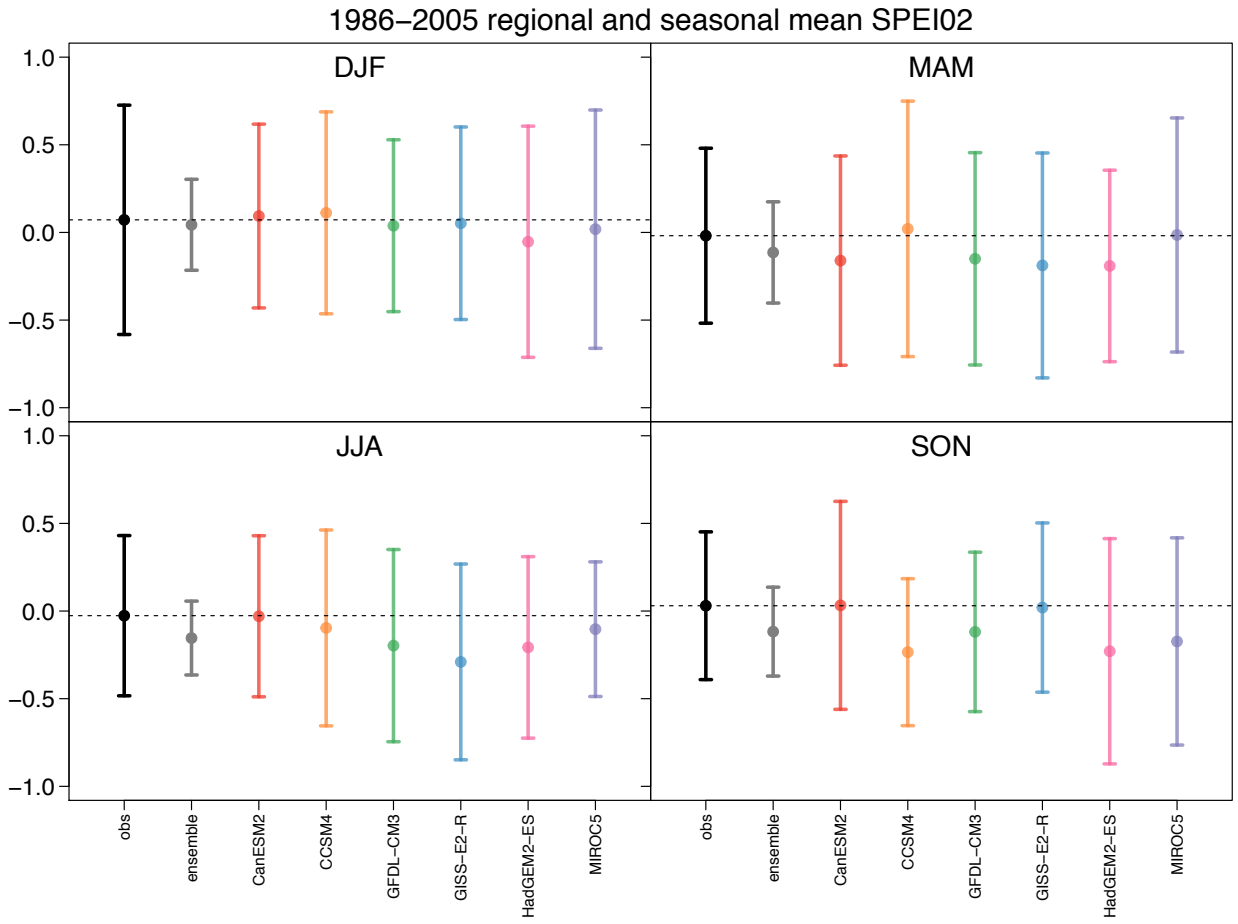

Figure S3. 1986-2005 seasonal mean and standard deviation of SPEI02 averaged over 117°-103°W, 28°-40°N, calculated from precipitation and temperature from observations (Livneh et al. [2015]; black) and six downscaled CMIP5 models (colored). The multi-model ensemble means are shown in grey.

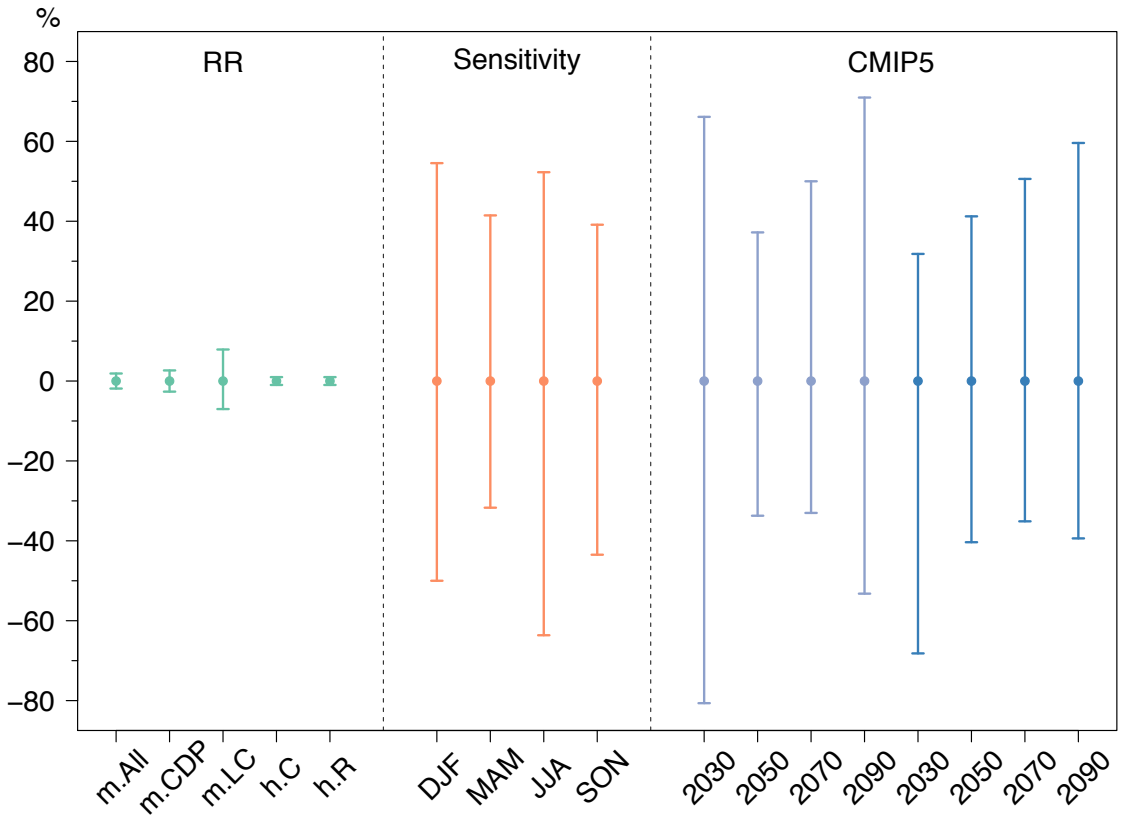

Figure S4. Comparison of influence of uncertainties and variability in input variables to the CRF (Equation 2) for fine dust. Left panel: 95% confidence interval of relative risks (RR) for all-cause (m.All), cardiopulmonary (m.CPD), lung cancer mortality (m.LC) and cardiovascular (h.C) and respiratory (h.R) hospitalization. Middle panel: 95% confidence interval of the fine dust-SPEI02 linear sensitivity by season. Right panel: Spread in the CMIP5 model projections of changes in fine dust concentrations under RCP4.5 (light blue) and RCP8.5 (dark blue) scenarios at 20-year averaged intervals centered around 2030, 2050, 2070, and 2090. The upper and lower limits are calculated as percentage differences relative to the central estimate of each category (i.e., central relative risk, mean slope, and multi-model mean value).

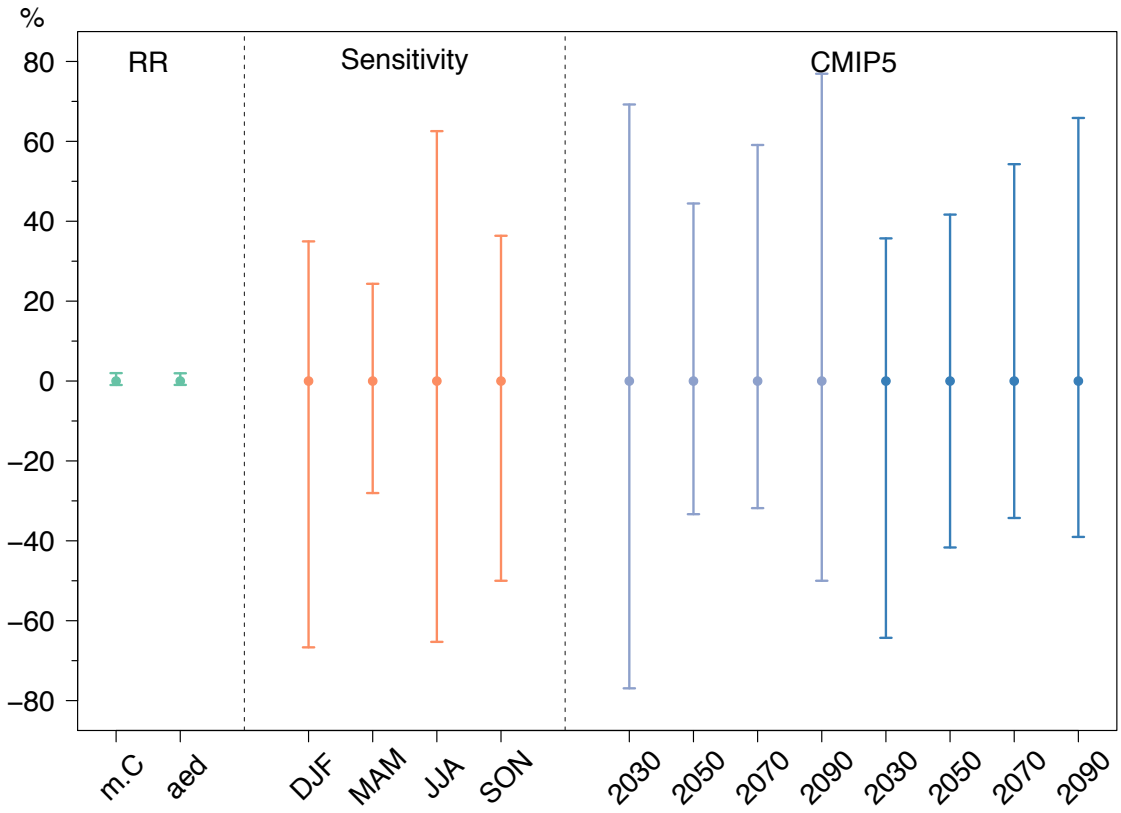

Figure S5. As in Figure S4 but for coarse dust. The health endpoints considered are cardiovascular mortality (m.C) and asthma ED visits (aed).

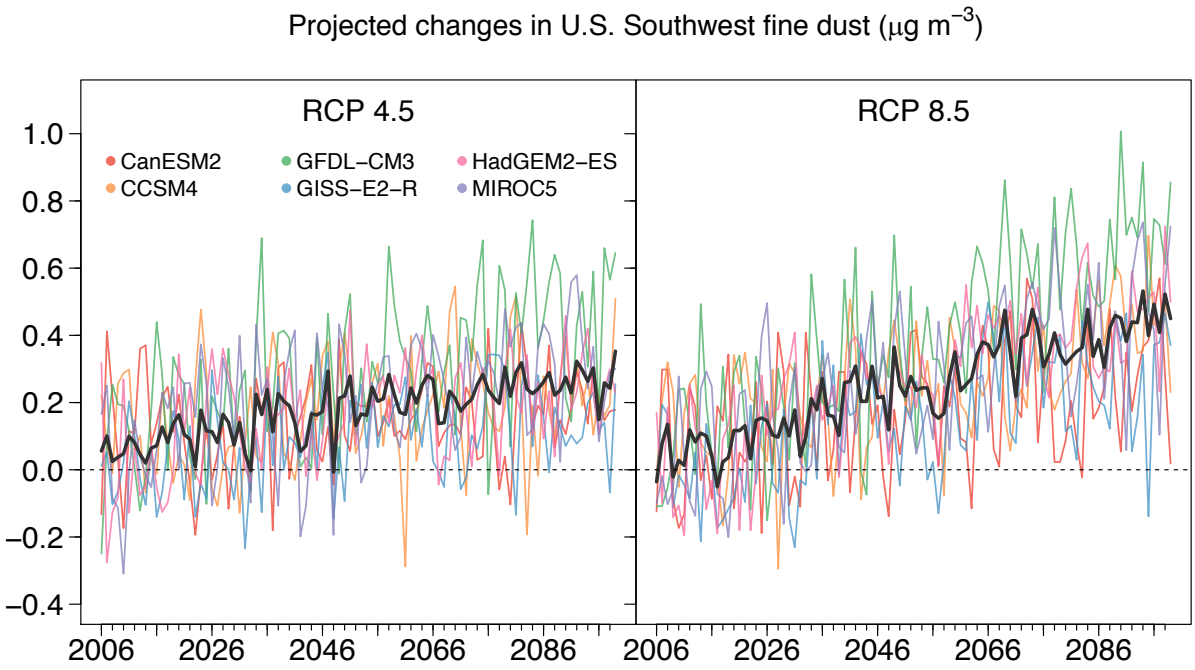

Figure S6. Projected changes in 2006-2099 fine dust averaged over the Southwest under RCP4.5 and RCP8.5 scenarios due to changes in the drought index, SPEI02. Annual mean changes are calculated relative to 1986-2005. Different colors represent results for individual CMIP5 models. The black lines show the multi-model means.

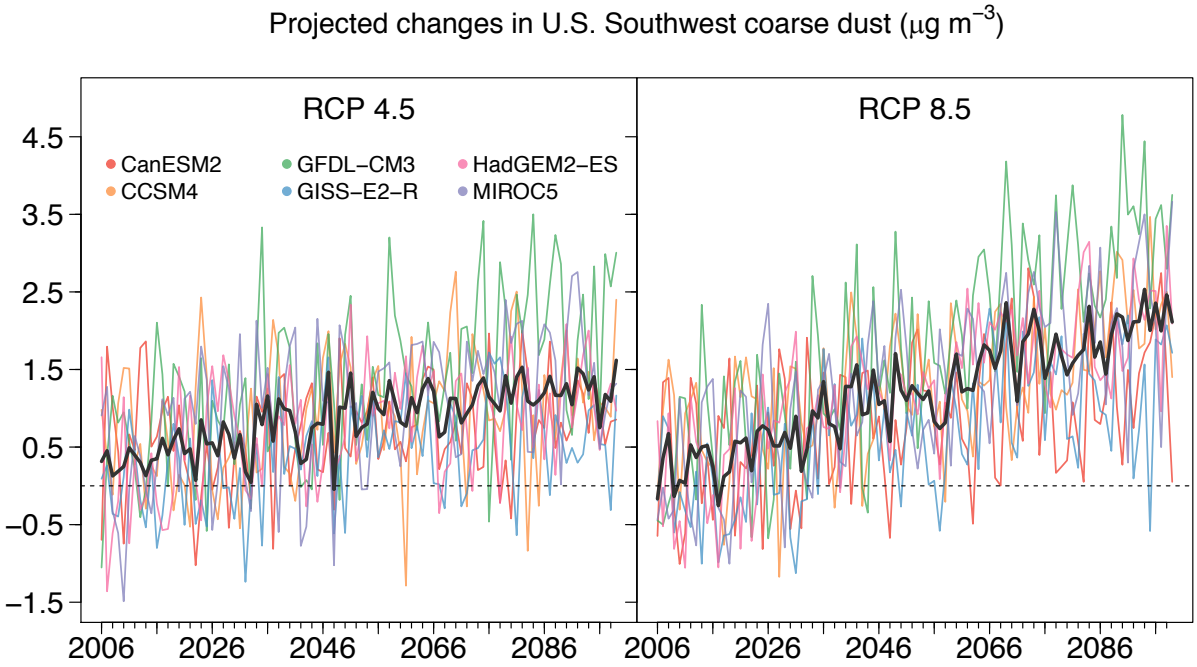

Figure S7. As in Figure S6 but for coarse dust.

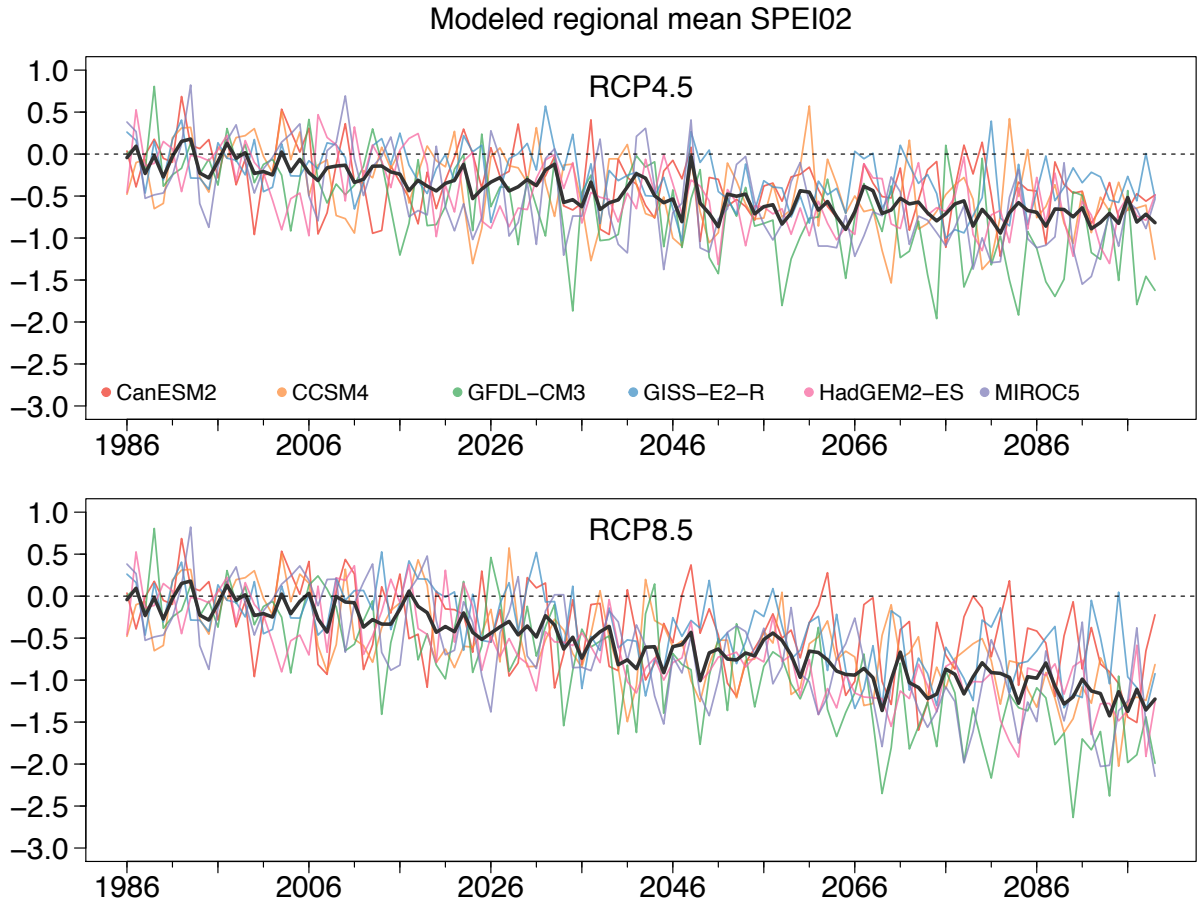

Figure S8. 1986-2099 timeseries of annual mean SPEI02 averaged over 28°-41°N and 117°-98°W for six different CMIP5 models under RCP4.5 (top) and RCP8.5 (bottom). The thick black lines show the multi-model means.

Table S1. Drought classification based on the Standardized Precipitation Evapotranspiration Index (SPEI). Sources: Dai et al., 2011; Liu et al., 2014; Törnros and Menzel, 2014.

SPEI values	**Drought/Flood classification**
$SPEI \leq -2$	Extremely dry
$-2 < SPEI \leq -1.5$	Severely dry
$-1.5 < SPEI \leq -1$	Moderately dry
$-1 < SPEI \leq 0$	Mild drought
$0 < SPEI \leq 1$	Near normal wet
$1 < SPEI \leq 1.5$	Moderately wet
$1.5 < SPEI \leq 2$	Very wet
$SPEI > 2$	Extremely wet

Table S2. Reference and projected population and total annual incidence. The population is the total projected population across the region for each health endpoint's associated age range. Total incidence is calculated using the projected county-level incidence rates multiplied by projected population disaggregated into 5-year age bins. Values are expressed in thousands and rounded to two significant figures.

			20-year era				
Pollutant	**Health Endpoint**		**2010**	**2030**	**2050**	**2070**	**2090**
Fine dust	Hospitalization, Cardiovascular less Myocardial Infarctions	Population (65-99 y)	2,100	4,100	5,300	6,000	6,600
		Total incidence	55	110	160	190	210
	Hospitalization, Non-fatal Acute Myocardial Infarction	Population (65-99 y)	2,100	4,100	5,300	6,000	6,600
		Total incidence	11	23	32	37	41
	Hospitalization, Respiratory	Population (65-99 y)	2,100	4,100	5,300	6,000	6,600
		Total incidence	51	100	150	170	190
	Mortality, All-cause	Population (30-99 y)	9,400	12,000	14,000	15,000	16,000
		Total incidence	120	170	240	290	320
	Mortality, Cardiopulmonary	Population (30-99 y)	9,400	12,000	14,000	15,000	16,000
		Total incidence	51	69	100	120	140
	Mortality, Lung Cancer	Population (30-99 y)	9,400	12,000	14,000	15,000	16,000
		Total incidence	6.2	8	8.9	9.5	11
Coarse dust	Emergency Department Visits, Asthma	Population (0-99 y)	16,000	19,000	22,000	24,000	26,000
		Total incidence	74	84	95	110	110
	Mortality, Cardiovascular*	Population (0-99 y)	16,000	19,000	22,000	24,000	26,000
		Total incidence	51	69	100	120	140

*Cardiovascular mortality endpoint approximated from cardiopulmonary incidence (note that when rounded to 2 s.f., the incidence appears to be the same for the 30-99 and 0-99 year age groups).

Table S3. List of relative risk values for different health endpoints associated with $PM_{2.5}$ exposure used in this study.

Health Endpoint	**Epidemiological study**	**Cohort age (years)**	**Cohort location**	**Relative risk per 10 µg m^{-3} (95% CI)**	**Function type**
Mortality, all-cause	Krewski et al. (2009)	30-99	US nationwide	1.06 (1.04-1.08)	Log-linear
Mortality, cardiopulmonary				1.13 (1.10-1.16)	Log-linear
Mortality, lung cancer				1.14 (1.06-1.23)	Log-linear
Hospital admissions, all cardiovascular (less myocardial infarction)	Zanobetti et al. (2009)	65-99	26 US communities	1.02 (1.01-1.03)	Log-linear
Hospital admissions, respiratory				1.02 (1.01-1.03)	Log-linear
Hospital admissions, non-fatal acute myocardial infarction	Peters et al. (2001)	65-99	Boston, MA	1.62 (1.13-2.34)	Logistic

Table S4. List of relative risk values for different health endpoints associated with $PM_{2.5-10}$ exposure used in this study.

Health Endpoint	**Epidemiological study**	**Cohort age (years)**	**Cohort location**	**Relative risk per 10 µg m^{-3} (95% CI)**	**Function type**
Mortality, cardiovascular	Malig and Ostro (2009)	0-99	Multiple cities, CA	1.01 (1.00-1.03)	Logistic
Emergency department visits, asthma	Malig et al. (2013)	0-99	Multiple cities, CA	1.03 (1.02-1.05)	Logistic

Table S5. Percent of incidence attributable to each age group by health endpoint and 20-year era. The percentages are calculated by dividing the estimated incidence associated with each age group by the total annual incidence found in Table S2.

			20-year era			
Pollutant	**Health Endpoint**	**Age group (years)**	**2030**	**2050**	**2070**	**2090**
Fine Dust	Mortality, all-cause*	30-74	29%	16%	12%	12%
		75-99	71%	84%	88%	88%
Coarse Dust	Emergency department visits, asthma	0-17	37%	37%	36%	36%
		18-74	56%	54%	54%	54%
		75-99	7%	9%	10%	11%
	Mortality, cardiovascular	0-17	0.1%	0.1%	< 0.1%	< 0.1%
		18-74	22%	12%	9%	9%
		75-99	78%	88%	91%	91%

*All-cause mortality was only calculated for ages 30-99, as age is restricted by the underlying epidemiological study.

Table S6. Annual economic damages (millions USD 2015$) associated with the health burdens in Table 2. The historical reference value is estimated using 2010 population and baseline incidence rates combined with 1988-2005 dust concentrations. Values shown for future scenarios at 20-year intervals are the excess cost relative to the reference value. "AQ-constant" projections are due to the effects of changing population and baseline incidence rates. RCP projections are due to the combined effects of changing dust concentrations, population, and baseline incidence rates. For each health endpoint and 20-year era, the total cost is equal to the sum of the reference and excess costs projected for each future scenario. Values in parentheses represent the range of variability in the CMIP5 model ensemble for a given RCP scenario. Values are rounded to two significant figures.

Pollutant	Health endpoint	Age (years)	Reference value (per year)		20-year averaged excess damage relative to reference (per year)			
				Scenario	2030	2050	2070	2090
Fine dust	Hospitalization, Cardiovascular less Myocardial Infarctions	65-99	5.7	AQ constant	4.8	9.3	12	14
				RCP4.5	6.0 (5.1,6.8)	12 (11,13)	15 (14,19)	18 (16,22)
				RCP8.5	6.0 (5.3,6.5)	12 (11,14)	17 (16,20)	21 (18,25)
	Hospitalization, Non-fatal Acute Myocardial Infarction	65-99	38	AQ constant	32	60	75	87
				RCP4.5	40 (34,46)	75 (70,83)	97 (90,110)	120 (100,140)
				RCP8.5	40 (35,44)	80 (72,90)	110 (98,130)	130 (120,160)
	Hospitalization, Respiratory	65-99	4.7	AQ constant	4	7.7	9.8	11
				RCP4.5	5.0 (4.2,5.7)	9.7 (9.0,11)	13 (12,14)	15 (13,18)
				RCP8.5	5.0 (4.4,5.5)	10 (9.2,11)	14 (13,17)	17 (15,21)
	Mortality, All-cause	30-99	8200	AQ constant	4800	10000	15000	19000
				RCP4.5	6300 (5100,7200)	13000 (12000,15000)	20000 (19000,23000)	27000 (23000,32000)
				RCP8.5	6300 (5400,6900)	14000 (13000,16000)	23000 (20000,27000)	31000 (20000,38000)
	Mortality, Cardiopulmonary	30-99	7400	AQ constant	3300	8800	13000	18000
				RCP4.5	4500 (3600,5300)	12000 (11000,13000)	18000 (16000,20000)	25000 (21000,30000)

				RCP8.5	4600 (3800,5100)	12000 (11000,14000)	20000 (18000,24000)	29000 (24000,36000)
	Mortality, Lung Cancer	30-99	1000	AQ constant	420	640	820	1200
				RCP4.5	570 (460,670)	900 (820,1000)	1200 (1100,1400)	1800 (1500,2200)
				RCP8.5	580 (480,640)	990 (840,1100)	1400 (1200,1800)	2100 (1700,2600)
Coarse dust	Emergency Department Visits, Asthma	0-99	0.85	AQ constant	0.11	0.23	0.35	0.40
				RCP4.5	0.19 (0.13,0.25)	0.36 (0.32,0.41)	0.56 (0.47,0.62)	0.62 (0.50,0.77)
				RCP8.5	0.20 (0.14,0.23)	0.40 (0.33,0.47)	0.63 (0.53,0.78)	0.75 (0.61,0.96)
	Mortality, Cardiovascular*	0-99	4500	AQ constant	2100	5600	8400	11000
				RCP4.5	2700 (2200,3100)	6900 (6500,7400)	11000 (9900,12000)	14000 (13000,16000)
				RCP8.5	2700 (2300,2900)	7400 (6700,8100)	12000 (11000,14000)	16000 (14000,19000)

Table S7. Sensitivity of VSL and total valuation estimates to alternative economic growth and income elasticity inputs (million 2015$).

Key Assumptions	2030	2050	2070	2090
With GDP/capita growth and income elasticity =0.4	$11.0	$12.4	$13.8	$15.2
With GDP/capita growth and income elasticity =1.0	$12.8	$17.3	$22.4	$28.4
Change based on alternative income elasticity	16%	39%	62%	87%